A Covariance-Based Realization Algorithm for the Identification of Aeroelastic Dynamics from In-Flight Data

Daniel N. Miller[*] and Raymond A. de Callafon[†]

University of California San Diego, La Jolla, CA

Martin J. Brenner[‡]

NASA Dryden Flight Research Center, Edwards, CA

The unsteady, aerodynamically induced resonance of aircraft structures may lead to potentially destructive vibrations when left unaccounted for in flight control system design. Such aeroelastic modes are difficult to accurately predict analytically, and computational models require calibration, verification, and validation. The successful design of control systems that actively suppress aeroelastic vibrations thus requires the capability to identify unbiased parametric estimates of aeroelastic resonance modes.

We present a novel subspace system identification method inspired by covariance estimates and classical realization techniques that constructs system estimates from measured input-output data. The resulting covariance-based realization algorithm allows for the identification of parametric system models from data sets of large signal dimension and is applicable to data perturbed by colored noise and acquired in closed-loop operation due to the unbiased estimation of cross-covariance functions, even in low signal-to-noise conditions.

The algorithm is applied to data measured on board the **NASA Active Aeroelastic Wing F/A-18**. The results demonstrate the effectiveness of the algorithm in efficiently computing accurate, unbiased linear dynamic models

---

[*]Graduate Student, Dept. of Mechanical and Aerospace Engineering, d6miller@ucsd.edu, Student Member AIAA.

[†]Professor, Dept. of Mechanical and Aerospace Engineering, callafon@ucsd.edu.

[‡]Aerospace Engineer, martin.j.brenner@nasa.gov, Senior Member AIAA.

from large data sets of high-dimensional signal sets obtain from aircraft in flight.

I.   Introduction

Vibrations due to aero-servo-elastic (ASE) dynamics of aircraft structures, commonly referred to as flutter, have the potential to damage and destroy aircraft in flight if not properly analyzed and suppressed. The current trend in the analysis of ASE dynamics is to derive finite-element and computational-fluid-dynamic models of an airframe at various flight conditions, and to interpolate and extrapolate the damping of flutter modes across the full flight envelope. These computational models are then validated through ground testing and, finally, in-flight testing before the aircraft can be considered operationally safe.[1]

In-flight analysis of flutter, however, is inherently difficult due not only to its dangerous nature, but also to the unsteady, turbulent phenomena that induce it. These effects manifest themselves as essentially non-deterministic disturbances, or noise, on acquired data. By nature this noise is colored and correlated across all measured signals; perturbations on control surface positions due to turbulent air flow are inherently correlated with the perturbations measured in stress and acceleration on the aircraft. Attempts to analyze data generated from in-flight experiments must take these facts into account to avoid inaccurate conclusions.

System identification is the discipline of constructing dynamic models from experimental data. Most identification methods assume that the noise on measured signals is either white, uncorrelated, or both, and are thus ill-suited for identifying ASE dynamics. When dealing with experimental data that does not meet these assumptions, techniques from the analysis of stochastic processes must be incorporated into the identification methods used. Additionally, many system identification methods are based on nonlinear optimizations over cost functions that become extremely non-convex for large, high-dimensional data sets, making them infeasible for ASE analysis, in which many sensors are employed to capture the behavior of the airframe.

Traditional subspace methods[2] have been previously applied to the identification of aeroelastic dynamics using simulated data from an F-16 aircraft and measured data from a V-22 rotocraft.[3] Such methods assume strictly deterministic inputs in order to remove the effects of subsequent input on the propagation of the state dynamics and in order to de-correlate the deterministic and non-deterministic subsystems. A subspace-based method for online monitoring of aeroelastic damping was developed and applied to in-flight data by Mevel et al.[4] This method utilized output data only and relied on the auto-covariance of the data to determine when statistically-significant damping of vibration modes dropped below a given threshold. It did not, however, identify the input-output behavior of the aeroelastic phenom-

ena and assumed no deterministic control-surface excitation during data acquisition. This method was later extended to include known, strictly-deterministic inputs.[5]

These previous studies all assume disturbances to be white, which in practice is often insufficient. Non-deterministic effects from turbulence, sensor noise, and, in the closed-loop case, control-system feedback will inevitably produce colored noise on the output data. In such cases, either the modes of the estimated system will be biased by the disturbance spectrum,[6] or, if the model-order is chosen to be artificially high, the observable modes of the strictly non-deterministic subsystem will be estimated along-side the modes of the deterministic subsystem but be incorrectly identified as controllable.[7] This is particularly problematic if the dynamic model is intended to be used for active flutter suppression, as the control algorithm designed from the derived model will attempt to control the uncontrollable modes. Additionally, treatment of the input as strictly deterministic is only possible if the input measured is actuator commands. In this case, the derived model will include actuator dynamics (such as servomotor dynamics) as well as aeroelastic dynamics. If actuator positions are measured instead, the position measurements will include perturbations which are correlated with the noise on the measured output data, and the effects of the input on state-dynamics cannot be removed with the standard methods of orthogonal projections.

Alternative proposed methods of estimating ASE dynamics include applying frequency-domain total-least-squares by restricting the identification to error-in-variables models,[8] which allows for the incorporation of colored noise. An approach based on rational orthogonal basis functions incorporated static input and output nonlinearities and addressed the issue of identifying parameter-varying models.[9] Neither allows for the presence of correlated noise on both the input and output measurements, and unlike subspace methods, these methods all require *a priori* parameterization of the dynamic system.

The goal of the material presented herein is to advance the state of in-flight aeroelastic analysis by describing a system identification method that computes a linear dynamic system of aeroelastically-induced vibration modes in the presence of colored and correlated noise on both input and output measurements while remaining scalable to large, high-dimensional data sets. The method uses estimated cross-covariance functions between signals to reduce the effects of noise and focus on only the input-output behavior of a system. The result is a subspace identification algorithm that generalizes realization theory by incorporating results from stochastic processes and is thereby referred to as a Covariance-Based Realization Algorithm (CoBRA) by the authors. The algorithm possesses resemblance to and inspiration from the Eigensystem Realization Algorithm[10] and the commonly associated Observer / Kalman Filter Identification (OKID),[11] identification methods used frequently in the aerospace community.

The following section of the paper describes the algorithm in detail and discusses its re-

lationship to other identification methods. The algorithm is then applied to data measured from in-flight experiments performed with the NASA F/A-18 Active Aeroelastic Wing aircraft, which includes a discussion of the various sources of bias that would result were the identification to be performed from the input-output data alone. It is shown that CoBRA is effective in modeling induced vibration modes for in-flight experiments. Results and future work are discussed in the conclusion.

II.   Identification from Dynamic Invariance

This section describes the algorithm to be later applied to the identification of ASE dynamics. After a preliminary background on stochastic processes necessary to define notation and assumptions on the measured signals, we demonstrate how shifted data matrices can be used to estimate the discrete-time invariant dynamics responsible for propagating the state over samples of measured data, followed by a discussion of the relationship between the algorithm and other subspace identification methods. Finally, it is shown that when a purely white-noise input is used and the covariance function estimates computed over a specific domain, the algorithm asymptotically generalizes to the well-known Eigensystem Realization Algorithm.

II.A.   Preliminary Theory of Stochastic Processes

Before presenting the proposed identification framework, we review some key results of stochastic processes and linear systems. In the following, the time signal t is assumed to be an integer index rather than a continuous time signal.

A signal $s(t) \in \mathbb{R}^{n_s}$ is said to be *quasi-stationary* if it satisfies the two conditions

$$Es(t) = m_s(t), \qquad ||m_s(t)||_2 \leq C \ \forall \ t \in \mathbb{Z} \tag{1}$$

and

$$R_s(\tau) = \lim_{N \to \infty} \frac{1}{N} \sum_{t=0}^{N} Es(t+\tau)s(t)^T, \quad \forall \tau \in \mathbb{Z}, ||R_s(\tau)||_2 \leq C, \tag{2}$$

for some $C < \infty$, where E denotes expectation, which has no effect if $s(t)$ is strictly deterministic. The function $R_s(\tau) : \mathbb{Z} \to \mathbb{R}^{n_s \times n_s}$ is called the *autocovariance function* of $s(t)$. Similarly, if $w(t) \in \mathbb{R}^{n_w}$ is a second quasi-stationary signal, then the function $R_{sw}(\tau) : \mathbb{Z} \to \mathbb{R}^{n_s \times n_w}$,

$$R_{sw}(\tau) = \lim_{N \to \infty} \frac{1}{N} \sum_{t=0}^{N} Es(t+\tau)w(t)^T$$

is called the *cross-covariance* function of $s(t)$ and $w(t)$. If only N samples of data are

available, the autocovariance and cross-covariance function estimates

$$\hat{R}_s(\tau) = \frac{1}{N} \sum_{t=0}^{N} s(t+\tau)s(t)^T$$

$$\hat{R}_{sw}(\tau) = \frac{1}{N} \sum_{t=0}^{N} s(t+\tau)w(t)^T$$

(3)

converge to $R_s(\tau)$ and $R_{sw}(\tau)$, respectively, as $N \to \infty$.[12] In this paper, all signals are restricted to being quasi-stationary and zero mean.

Next, consider a linear, time-invariant, discrete-time system described by the state-space equations

$$x(t+1) = Ax(t) + Bu(t)$$

$$y(t) = Cx(t) + Du(t) + v(t),$$

(4)

which relate the input $u(t) \in \mathbb{R}^{n_u}$ to the state $x(t) \in \mathbb{R}^n$ and the output $y(t) \in \mathbb{R}^{n_y}$ in terms of the constant matrices $A \in \mathbb{R}^{n \times n}$, $B \in \mathbb{R}^{n \times n_u}$, $C \in \mathbb{R}^{n_y \times n}$, and $D \in \mathbb{R}^{n_y \times n_u}$. Added to the output is a possibly-colored noise signal $v(t) \in \mathbb{R}^{n_y}$, assumed to be the realization of a stationary, stochastic process that may or may not share dynamics with the system described by (A, B, C, D). We limit (4) to include only minimal realizations[13] of stable systems.

If $u(t)$ is selected to be quasi-stationary, then the stationary property of $v(t)$ will result in a quasi-stationary $y(t)$.[12] If $\xi(t) \in \mathbb{R}^{n_\xi}$ is some quasi-stationary signal that is correlated with $u(t)$ and $v(t)$, then the cross-covariance functions $R_{u\xi}(\tau) \in \mathbb{R}^{n_u \times n_\xi}$, $R_{y\xi}(\tau) \in \mathbb{R}^{n_y \times n_\xi}$, and $R_{v\xi}(\tau) \in \mathbb{R}^{n_y \times n_\xi}$ will exist. If we define the cross-covariance of the state with $\xi(t)$ as $R_{x\xi}(\tau) \in \mathbb{R}^{n \times n_\xi}$, then the covariance functions may be expressed in terms of the state-space matrices (A, B, C, D) as

$$R_{x\xi}(\tau+1) = AR_{x\xi}(\tau) + BR_{u\xi}(\tau)$$

$$R_{y\xi}(\tau) = CR_{x\xi}(\tau) + DR_{u\xi}(\tau) + R_{v\xi}(\tau).$$

(5)

If, however, $\xi(t)$ is chosen such that it is correlated with $u(t)$ but uncorrelated with $v(t)$, then

$$R_{v\xi}(\tau) = 0 \quad \forall \quad \tau,$$

(6)

and the relationship between $R_{u\xi}(\tau)$ and $R_{y\xi}(\tau)$ will be limited to the dynamics of the deterministic subsystem. Examples of such $\xi(t)$ include $u(t)$ itself if the input data is unperturbed and in open-loop operation, or an external reference signal if the data is measured in closed-loop operation.[12]

In this paper, it will always be assumed that $u(t)$ is quasi-stationary, that $v(t)$ is station-

ary; thus $y(t)$ is quasi-stationary and zero-mean due to the previously assumed stability of A.

II.B.   Identification from Dynamic Invariance of covariance functions

Subspace identification refers to a broad class of system identification methods that estimate system dynamics without the need for iterative or nonlinear numerical tools. The general approach of such methods is to estimate state-space system parameters from the row space of some alternative matrix constructed from measured data. Although some notable exceptions exist, by far the most common approach, and the one used in this paper, is to construct block-Hankel matrices of measured data, then use various projection operations to isolate the free-response of the system at subsequent time steps.[2]

The algorithm proposed in this paper differs from classical subspace algorithms in two critically significant ways: we propose to solve for the system dynamics based on variation of covariance-function estimates, and we solve for the system matrices based not on the shift-invariance of the extended observability matrix, but on the one-time-step variation of the measured data. Before defining the latter value precisely, we first review some of the data-matrix equations central to subspace methods.

Let $\hat{R}_{y\xi}(\tau)$ be an estimate of the cross-covariance function $R_{y\xi}(\tau)$, as defined in (3), computed over some domain $\tau \in [\tau_{\min}, \tau_{\max}]$. A block-Hankel matrix consisting of l block columns of i length sequences of $\hat{R}_{y\xi}(\tau)$

$$\mathbf{R}_{y\xi} = \begin{bmatrix} \hat{R}_{y\xi}(\tau_{\min}) & \hat{R}_{y\xi}(\tau_{\min}+1) & \cdots & \hat{R}_{y\xi}(\tau_{\min}+l-1) \\ \hat{R}_{y\xi}(\tau_{\min}+1) & \hat{R}_{y\xi}(\tau_{\min}+2) & \cdots & \hat{R}_{y\xi}(\tau_{\min}+l) \\ \vdots & \vdots & & \vdots \\ \hat{R}_{y\xi}(\tau_{\min}+i-1) & \hat{R}_{y\xi}(\tau_{\min}+i) & \cdots & \hat{R}_{y\xi}(\tau_{\min}+i+l-2) \end{bmatrix} \in \mathbb{R}^{in_y \times ln_\xi}$$

may be expressed as

$$\mathbf{R}_{y\xi} = \Gamma \mathbf{R}_{x\xi} + T\mathbf{R}_{u\xi} + \mathbf{R}_{v\xi}, \tag{7}$$

in which

$$\Gamma = \begin{bmatrix} C^T & (CA)^T & (CA^2)^T & \cdots & (CA^{i-1})^T \end{bmatrix}^T \in \mathbb{R}^{in_y \times n} \tag{8}$$

is the extended observability matrix,

$$\mathbf{R}_{x\xi} = \begin{bmatrix} \hat{R}_{x\xi}(\tau_{\min}) & \hat{R}_{x\xi}(\tau_{\min}+1) & \cdots & \hat{R}_{x\xi}(\tau_{\min}+l-1) \end{bmatrix} \in \mathbb{R}^{n \times ln_\xi}$$

is the propagation of cross-covariance of the state $x(t)$ with $\xi(t)$,

$$
T = \begin{bmatrix} G(0) & & & \\ G(1) & G(0) & & \\ \vdots & \vdots & \ddots & \\ G(i-1) & G(i-2) & \cdots & G(0) \end{bmatrix} \in \mathbb{R}^{in_y \times in_u} \tag{9}
$$

is a block-lower-triangular-Toeplitz matrix of the system Markov parameters

$$
G(k) = \begin{cases} 0, & k < 0, \\ D, & k = 0, \\ CA^{k-1}B, & k > 0, \end{cases}
$$

$$
\mathbf{R}_{u\xi} = \begin{bmatrix} \hat{R}_{u\xi}(\tau_{\min}) & \hat{R}_{u\xi}(\tau_{\min}+1) & \cdots & \hat{R}_{u\xi}(\tau_{\min}+l-1) \\ \hat{R}_{u\xi}(\tau_{\min}+1) & \hat{R}_{u\xi}(\tau_{\min}+2) & \cdots & \hat{R}_{u\xi}(\tau_{\min}+l) \\ \vdots & \vdots & & \vdots \\ \hat{R}_{u\xi}(\tau_{\min}+i-1) & \hat{R}_{u\xi}(\tau_{\min}+i) & \cdots & \hat{R}_{u\xi}(\tau_{\min}+i+l-2) \end{bmatrix} \in \mathbb{R}^{in_u \times ln_\xi}
$$

is a block-Hankel matrix of the cross-covariance of the input $u(t)$ and $\xi(t)$, and

$$
\mathbf{R}_{v\xi} = \begin{bmatrix} \hat{R}_{v\xi}(\tau_{\min}) & \hat{R}_{v\xi}(\tau_{\min}+1) & \cdots & \hat{R}_{v\xi}(\tau_{\min}+l-1) \\ \hat{R}_{v\xi}(\tau_{\min}+1) & \hat{R}_{v\xi}(\tau_{\min}+2) & \cdots & \hat{R}_{v\xi}(\tau_{\min}+l) \\ \vdots & \vdots & & \vdots \\ \hat{R}_{v\xi}(\tau_{\min}+i-1) & \hat{R}_{v\xi}(\tau_{\min}+i) & \cdots & \hat{R}_{v\xi}(\tau_{\min}+i+l-2) \end{bmatrix} \in \mathbb{R}^{in_y \times ln_\xi}
$$

is a block-Hankel matrix of the cross-covariance of the noise $v(t)$ and $\xi(t)$.

Define the shifted $\mathbf{R}_{y\xi}$ as

$$
\overline{\mathbf{R}}_{y\xi} = \begin{bmatrix} \hat{R}_{y\xi}(\tau_{\min}) & \hat{R}_{y\xi}(\tau_{\min}+1) & \cdots & \hat{R}_{y\xi}(\tau_{\min}+l-1) \\ \hat{R}_{y\xi}(\tau_{\min}+1) & \hat{R}_{y\xi}(\tau_{\min}+2) & \cdots & \hat{R}_{y\xi}(\tau_{\min}+l) \\ \vdots & \vdots & & \vdots \\ \hat{R}_{y\xi}(\tau_{\min}+i-1) & \hat{R}_{y\xi}(\tau_{\min}+i) & \cdots & \hat{R}_{y\xi}(\tau_{\min}+i+l-2) \end{bmatrix} \in \mathbb{R}^{in_y \times ln_\xi}.
$$

This may be expressed as

$$
\overline{\mathbf{R}}_{y\xi} = \Gamma A \mathbf{R}_{x\xi} + T^+ \mathbf{R}_{u\xi}^+ + \overline{\mathbf{R}}_{v\xi}, \tag{10}
$$

in which

$$T^+ = \begin{bmatrix} G(1) \\ \vdots & & T \\ G(i) \end{bmatrix} \in \mathbb{R}^{in_y \times (i+1)n_u}$$

is the block-Toeplitz matrix of Markov parameters T extended by one block column and

$$\mathbf{R}_{u\xi}^+ = \left[\begin{array}{ccc} & \mathbf{R}_{u\xi} & \\ \hline \hat{R}_{u\xi}(\tau_{\min} + i) & \cdots & \hat{R}_{u\xi}(\tau_{\min} + i + l - 1) \end{array} \right] \in \mathbb{R}^{(i+1)n_u \times ln_\xi}$$

is the block-Hankel matrix $\mathbf{R}_{u\xi}$ extended by one block row.

Our goal is to estimate the parameter A that appears in (10). Doing so requires isolating the row space of Γ by removing the row spaces of T and T^+ in (7) and (10), respectively. Define the projector matrix

$$\Pi = I_{ln_\xi} - (\mathbf{R}_{u\xi}^+)^T \left((\mathbf{R}_{u\xi}^+)(\mathbf{R}_{u\xi}^+)^T \right)^{-1} \mathbf{R}_{u\xi}^+ \in \mathbb{R}^{ln_\xi \times ln_\xi}.$$

This projector has the property[7]

$$\mathbf{R}_{u\xi}\Pi = 0_{in_u \times ln_\xi}$$
$$\mathbf{R}_{u\xi}^+\Pi = 0_{(i+1)n_u \times ln_\xi}$$

so that multiplication of (7) and (10) on the right by Π results in

$$\mathbf{R}_{y\xi}\Pi = \Gamma A \mathbf{R}_{x\xi}\Pi + \mathbf{R}_{v\xi}\Pi$$

and

$$\overline{\mathbf{R}}_{y\xi}\Pi = \Gamma A \mathbf{R}_{x\xi}\Pi + \overline{\mathbf{R}}_{v\xi}\Pi,$$

respectively. A persistently exciting input signal is sufficient to preserve the row space of Γ in $\mathbf{R}_{y\xi}\Pi$ and $\overline{\mathbf{R}}_{y\xi}\Pi$.[6, 14]

We are now prepared to precisely define the identification procedure. Suppose that $\hat{\Gamma}$ is an estimate of Γ. Then the least-squares estimate of the state dynamics over one time step is

$$\begin{aligned} \hat{A} &= \arg\min_{\bar{A}} \left\| \bar{A}\hat{\Gamma}^\dagger \mathbf{R}_{y\xi}\Pi - \hat{\Gamma}^\dagger \overline{\mathbf{R}}_{y\xi}\Pi \right\|_F \\ &= \Gamma^\dagger \overline{\mathbf{R}}_{y\xi}\Pi \left(\Gamma^\dagger \mathbf{R}_{y\xi}\Pi \right)^\dagger, \end{aligned} \tag{11}$$

in which $(\cdot)^\dagger$ represents the Moore-Penrose pseudoinverse. If at first the estimate $\hat{A}$ appears

arbitrary, note that if Γ, $R_{y\xi}(\tau)$, and $R_{u\xi}(\tau)$ are known exactly, (11) reduces to

$$\hat{A} = \arg \min_{\bar{A}} \left|\left| \left(\bar{A} - A \right) \mathbf{R}_{x\xi} \Pi \right|\right|_F . \tag{12}$$

Hence the statement that (11) is a least-squares estimate of the propagation of $\hat{R}_{x\xi}(\tau)$ in one step of τ. Although there are several valid ways to find an estimate $\hat{\Gamma}$, we choose to employ the singular-value decomposition (SVD) of $\mathbf{R}_{y\xi} \Pi$ so that (11) reduces to a familiar closed-form expression.

To estimate Γ, first observe that $\mathrm{rank}(\Gamma) = n$. Hence

$$\mathrm{rank}(\mathbf{R}_{y\xi} \Pi - \mathbf{R}_{v\xi} \Pi) = n.$$

Thus we choose to look for the closest rank-n matrix to $\mathbf{R}_{y\xi} \Pi$ in a 2-norm sense, that is

$$\min_{Q} \left|\left| Q - \mathbf{R}_{y\xi} \Pi \right|\right|_2 . \tag{13}$$

Define the SVD

$$\mathbf{R}_{y\xi} \Pi = \begin{bmatrix} U_n & U_s \end{bmatrix} \begin{bmatrix} \Sigma_n & 0 \\ 0 & \Sigma_s \end{bmatrix} \begin{bmatrix} V_n^T \\ V_s^T \end{bmatrix} , \tag{14}$$

in which Σ_n is a diagonal matrix containing the first n singular values of $\mathbf{R}_{y\xi} \Pi$, and Σ_s contains the remaining $s = i n_y - n$ singular values. The solution to (13) is then[15]

$$Q = U_n \Sigma_n V_n^T .$$

Moreover, the error is given by

$$\sigma_{n+1} = \left|\left| U_n \Sigma_n V_n^T - \mathbf{R}_{y\xi} \Pi \right|\right|_2 .$$

Thus if the system order n is unknown, it may be estimated by examining the singular values of $\mathbf{R}_{y\xi} \Pi$ and searching for a significant drop-off.

Hence, we let $Q = \hat{\Gamma} \hat{\mathbf{R}}_{x\xi} \Pi$ be an estimate of $\mathbf{R}_{y\xi} \Pi$. $\hat{\Gamma}$ may then be taken from any valid-dimensioned factorization of Q. We choose the factorization

$$\hat{\Gamma} = U_n \Sigma^{1/2} \quad \hat{\mathbf{R}}_{x\xi} \Pi = \Sigma^{1/2} V_n^T . \tag{15}$$

With $\hat{\Gamma}$ taken from (15), (11) reduces to

$$
\begin{aligned}
\hat{A} &= \hat{\Gamma}^{\dagger} \overline{\mathbf{R}}_{y\xi} \Pi \left(\hat{\Gamma} \mathbf{R}_{y\xi} \Pi \right)^{\dagger} \\
&= \Sigma_n^{-1/2} U_n^T \overline{\mathbf{R}}_{y\xi} \Pi V_n \Sigma_n^{-1/2}.
\end{aligned}
\tag{16}
$$

With $\hat{C}$ an estimate of C taken from the first n_y rows of $\hat{\Gamma}$, B and D can be shown to be linear in the relationship between $R_{y\xi}(\tau)$ and $R_{u\xi}(\tau)$ and thus solvable via a linear least-squares problem.[12,16]

Many modifications of the classical subspace identification problem can be applied to the described algorithm with similar benefits, such as implementation of the projection by means of the LQ decomposition[6] and replacing the orthogonal projection with an oblique projection.[17]

II.C.   Relationship to Other Subspace Identification Methods

When the instrument $\xi(t)$ is chosen to be the input signal $u(t)$ or the composite signal $\xi(t) = [y^T(t)\ u^T(t)]^T$ the algorithm resembles the MOESP family of algorithms,[18] which can be shown to reduce to forming cross-covariance estimates between the output and input during the projection step.[19] However, because PI-MOESP, PO-MOESP, and their related variants, such as Robust N4SID[17],[20] rely on the null-space projection to de-correlate the noise from the output data, they will only produce unbiased estimates when the input is noise-free.[21] Additionally, the orthogonal projection must be replaced with an oblique projection to guarantee unbiased estimates in the case of colored output noise,[18] which effectively limits the size of the data matrices available for identification since some rows of the data matrices must be selected to construct an oblique subspace.

An extension of MOESP has been proposed in which the system is perturbed by input, output, and state noise, which may all be correlated, so long as all noise signals are white, and this approach may be extended to the closed-loop case.[21] If the input or output measurement noise is colored, however, the estimates will once again become biased. Moreover, few of the methods address the issue of bias on the estimates of B and D, which determine the location of the system zeros. Identification via covariance-function estimates inherently guarantees that the identification will be constrained to the deterministic content of the data for all linear, time-invariant systems. Additionally, because covariance-function estimates may be computed via the fast Fourier transform, effectively pre-averaging the data, the amount of data that can be used for estimation purposes dramatically increases.

II.D. Relationship to the Eigensystem Realization Algorithm

When the input data is purely white, the preceding algorithm can be shown to reduce to a realization algorithm from noise-corrupted Markov parameters due to the autocovariance function of the input approaching a unit impulse.[22]

To see this, let H be a block-Hankel matrix of system Markov parameters starting at $G(1)$,

$$H = \begin{bmatrix} G(1) & G(2) & G(3) & \cdots \\ G(2) & G(3) & G(4) & \cdots \\ \vdots & \vdots & \vdots & \\ G(i) & G(i+1) & G(i+2) & \cdots \end{bmatrix} \in \mathbb{R}^{in_y \times \infty},$$

and let $\overline{H}$ be a block-Hankel matrix of Markov parameters starting at $G(2)$,

$$\overline{H} = \begin{bmatrix} G(2) & G(3) & G(4) & \cdots \\ G(3) & G(4) & G(5) & \cdots \\ \vdots & \vdots & \vdots & \\ G(i+1) & G(i+2) & G(i+3) & \cdots \end{bmatrix} \in \mathbb{R}^{in_y \times \infty}.$$

The data-matrix equations (7) and (10) can be expressed as

$$\mathbf{R}_{y\xi} = H\mathbf{R}_{u\xi}^p + T\mathbf{R}_{u\xi} + \mathbf{R}_{v\xi}$$

and

$$\overline{\mathbf{R}}_{y\xi} = \overline{H}\mathbf{R}_{u\xi}^p + T^+\mathbf{R}_{u\xi}^+ + \overline{\mathbf{R}}_{v\xi},$$

respectively, where $\mathbf{R}_{u\xi}^p$ is a block-Toeplitz matrix of input data,

$$\mathbf{R}_{u\xi}^p = \begin{bmatrix} \hat{R}_{u\xi}(\tau_{\min}-1) & \hat{R}_{u\xi}(\tau_{\min}) & \cdots & \hat{R}_{u\xi}(\tau_{\min}+l-2) \\ \hat{R}_{u\xi}(\tau_{\min}-2) & \hat{R}_{u\xi}(\tau_{\min}-1) & \cdots & \hat{R}_{u\xi}(\tau_{\min}+l-3) \\ \hat{R}_{u\xi}(\tau_{\min}-3) & \hat{R}_{u\xi}(\tau_{\min}-2) & \cdots & \hat{R}_{u\xi}(\tau_{\min}+l-4) \\ \vdots & \vdots & & \vdots \end{bmatrix} \in \mathbb{R}^{\infty \times l}.$$

Suppose $u(t)$ is a noise-free, white-noise input, and let $\xi(t) = u(t-1)$. Then $\hat{R}_{u\xi}(\tau)$ will converge to a unit pulse at $\tau = -1$ as $N \to \infty$. Let $\tau_{\min} = 0$ and $i > n$. Then $\mathbf{R}_{y\xi} = 0$, $\Pi = I_l$, and $H\mathbf{R}_{u\xi}^p$ and $\overline{H}\mathbf{R}_{u\xi}^p$ become finite products with $\mathbf{R}_{u\xi}^p = I_l$. Hence

$$\mathbf{R}_{y\xi}\Pi = H$$
$$\overline{\mathbf{R}}_{y\xi}\Pi = \overline{H}.$$

Thus (16) will asymptotically become a construction of a state-space realization from estimates of Markov parameters by means of the singular-value decomposition, which is the ERA.[10]

III.   Identification of Aero-Servo-Elastic Dynamics

The described dynamic-invariance-based identification algorithm was applied to in-flight data taken from accelerometer and pressure measurements on the NASA Dryden AAW F/A-18. Applying the preceding algorithm to ASE dynamics requires careful selection of the instrument signal $\xi(t)$ to ensure that the system estimate is unbiased. If $\xi(t)$ is chosen incorrectly, the result may be biased by either the noise process or unwanted system dynamics.

In the following two sections, we apply CoBRA to two separate experiments performed during aeroelastic analysis of the AAW F/A-18. In the first experiment, the pathway between leading-edge flap (LEF) position measurements and airfame accelerometers and wing pressure sensors is identified. The LEF position data is corrupted by disturbances on the surfaces due to turbulent airflow across the wing, making unbiased input-output identification directly from raw data impossible. In the second experiment, the response to differential aileron position is measured. This experiment has the added complication of being performed in closed-loop, so that the aileron positions are perturbed not only by airflow but by the flight control system response to additional, correlated disturbances.

III.A.   Collective Leading-Edge Flap Excitation

As a fist example, consider the identification of the response from the LEF to the acceleration and pressure sensors. Signal pathways for the system are shown in Figure 1, in which G_{lef} is the collective LEF actuator dynamics and G the ASE dynamics of interest. The collective LEF position $u(t)$ is perturbed by a noise signal $v_{\mathrm{lef}}(t)$ that *must* be assumed correlated with the noise $v(t)$ on the acceleration and pressure measurements $y(t)$. The result is that identification directly from $u(t)$ to $y(t)$ will be biased by the cross-spectrum of the two noise signals, regardless of the identification algorithm used, unless steps are taken to de-correlate them from the measured data.
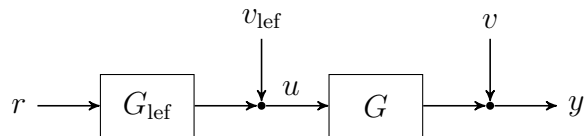

Figure 1. Leading-edge flap experiment signal pathways.

The OBES excitation $r(t)$ was chosen to be a minimax Crest factor multisine[23] of bandwidth between 3 Hz and 35 Hz. The power-spectral density (PSD) of the OBES signal is shown in Figure 2. It can be seen that $r(t)$ closely resembles white noise in the frequency range of interest. The OBES reference signal $r(t)$ is uncorrelated with either noise signal, since it is deterministic; it may also be treated as quasi-stationary, since as a sum of sinusoids, its autocovariance function exists. Hence the mapping between the cross-covariance functions $R_{yr}(\tau)$ and $R_{ur}(\tau)$ is limited to the dynamics G, and we select $\xi(t) = r(t)$ when analyzing the data.
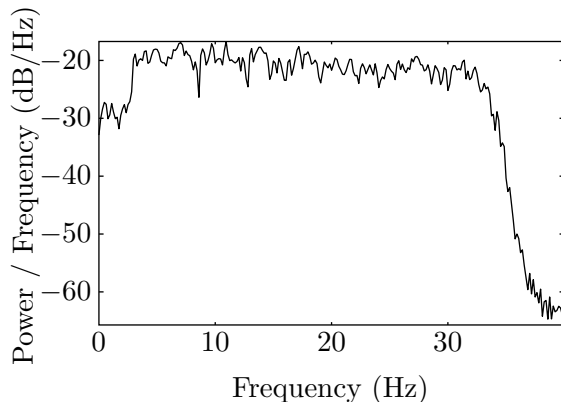
Figure 2. **Power-spectral density of OBES signal for collective LEF excitation.**

The estimated cross-covariance function of the input and reference $\hat{R}_{ur}(\tau)$ is shown in Figure 3. This can effectively be considered the covariance-function input into G. Only the data in which the excitation signal $r(t)$ is nonzero was used to calculate the PSD and cross-covariance functions. The cross-covariance functions were further truncated to $\tau \in [-20, 100]$ after calculation for identification purposes, since, as τ increases, the signal-to-noise ratio of the cross-covariance estimates becomes prohibitively small.
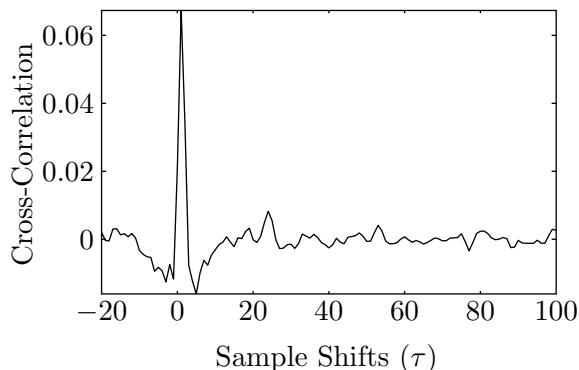
Figure 3. **Cross-covariance function estimate between collective LEF position (u) and OBES signal (r) for LEF excitation.**

Because 94 signals were available for use in identification, an objective, quantitative

criteria was created to determine which had a sufficiently high signal-to-noise ratio. Only signals which had magnitude-square coherence with the OBES of at least 2/3 averaged over the frequency range 3–35 Hz were selected from the available measurements. The locations of used and unused accelerometers are shown in Figure 4. Only the top-front-left pressure sensor was used. Although only 8 total signals were used for identification in this experiment, the collective LEF input is intended to excite neither rigid-body moments nor high-frequency bending moments on the wing, so the low number of usable signals is expected. Excitation of other surfaces will naturally produce different selections of signals for identification purposes.

A sample of signals measured for the experiment is shown in Figure 5 and their relative positions on the left wing of the aircraft in Figure 6. The samples marked with '*' did not meet the coherence criteria and were not used for identification purposes.
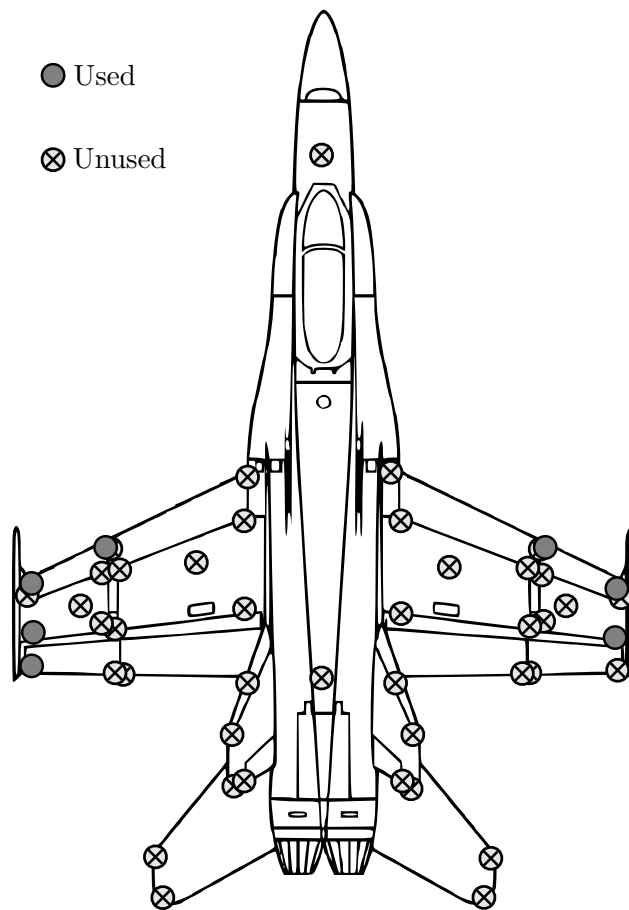
Figure 4. Locations of used and unused accelerometers for the collective LEF experiment.

A linear, state-space, discrete-time model was constructed from the measured data using the method proposed in Section II. The singular values of the projected data matrix (14) are shown in Figure 7. The system order was chosen to be $n = 4$. Time-domain simulations of the estimated model are shown with the measured data in Figure 8, in which the time-
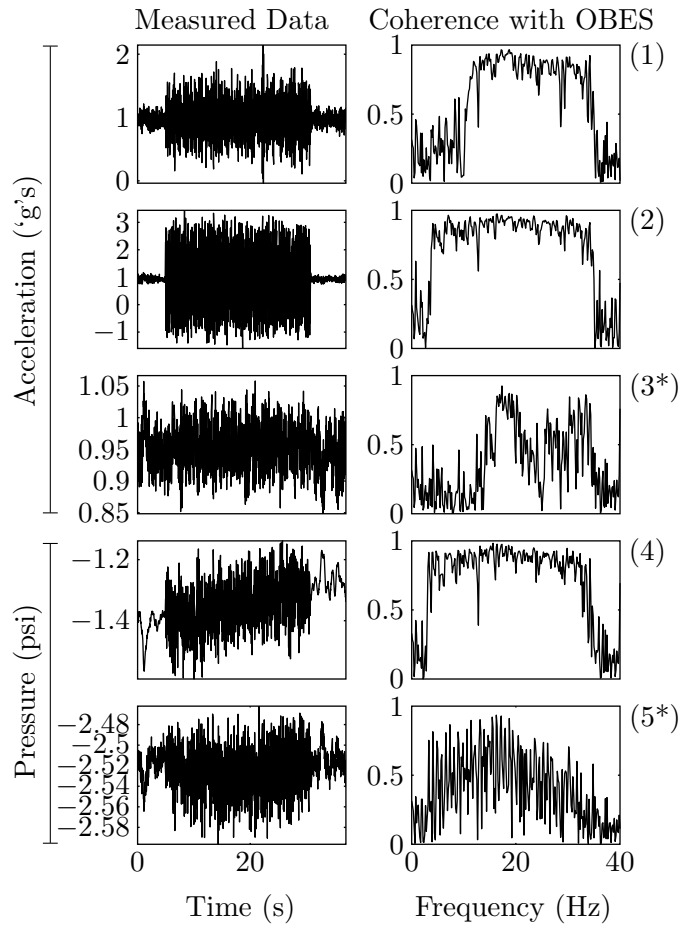
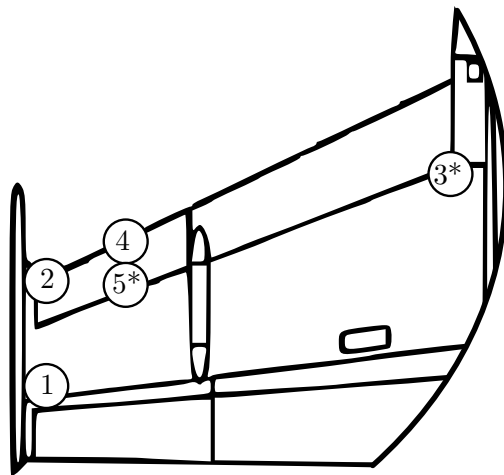**Figure 5. Sample of signals measured for the collective leading-edge flap experiment.**

Figure 6. Locations of sample signals for the collective LEF experiment.
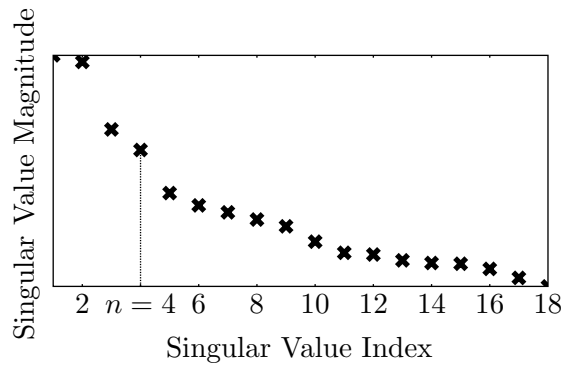
Figure 7. Singular values of the projected data matrix for the collective LEF experiment (y-axis in log scale).

domain measured data was de-trended before plotting. Cross-covariance estimates from the simulated data and measured data are shown in Figure 9. The units for the covariance function estimates are arbitrary due to the multiplication of measured data with the OBES signal.
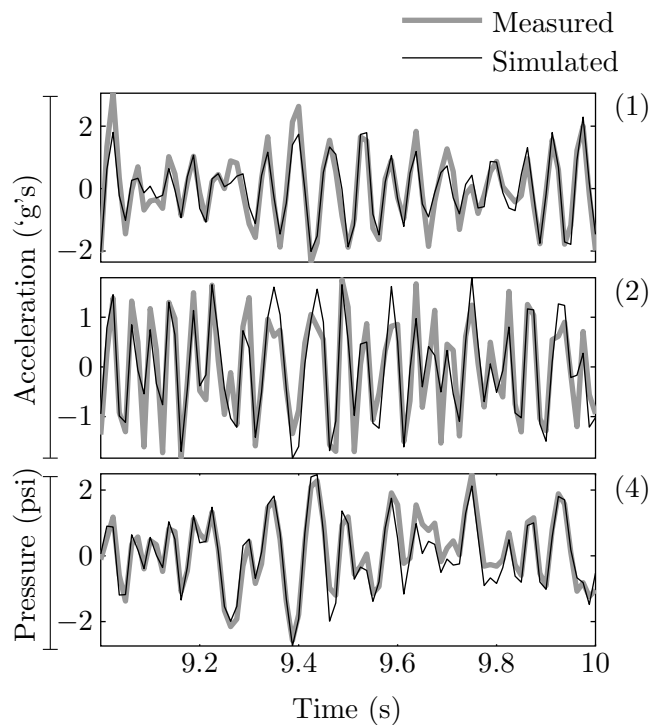
Figure 8. Sample of simulation results of the collective LEF experiment.

III.B. Differential Aileron Excitation

The second experiment examined is the identification of the response from the differential aileron input to the acceleration and pressure sensors. Signal pathways are shown in Figure
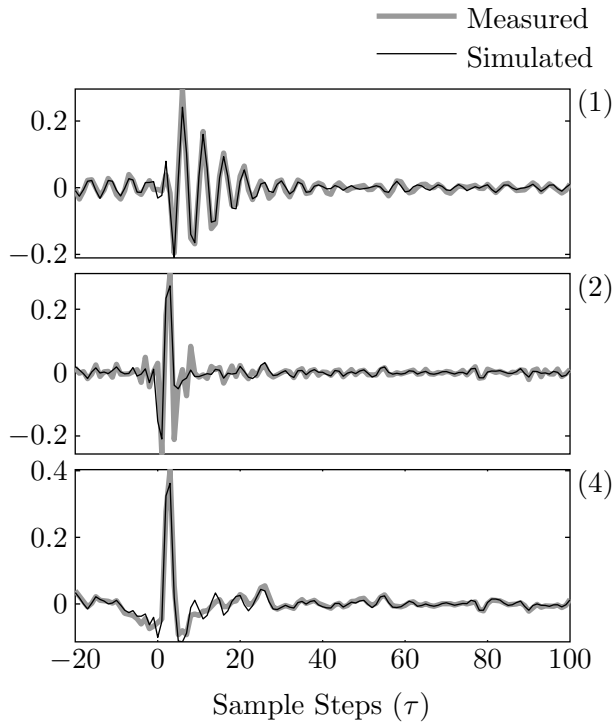
Figure 9. Sample of simulation cross-covariance estimates of the collective LEF experiment.

10. As before, the input $u(t)$ is perturbed by a noise signal $v_{\text{ail}}(t)$ and the output $y(t)$ by a noise signal $v(t)$. Additionally, the system contains a feedback controller C, which augments the excitation $r(t)$ with a differential aileron command. The feedback signals to the control system $y_C(t)$ are the result of both rigid-body and ASE dynamics, represented in a combined system G_C. The feedback $y_C(t)$ also contains a noise signal $v_C(t)$, which must be assumed correlated with $v_{\text{ail}}(t)$ and $v(t)$.
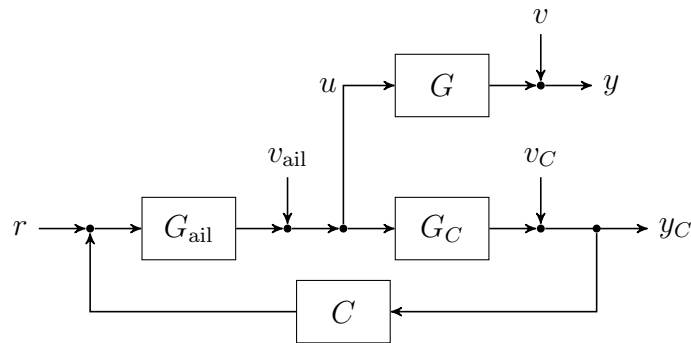

Figure 10. Aileron experiment signal pathways.

Because $v_C(t)$ appears in the input $u(t)$ after being filtered through the dynamics of G_C, C and the aileron servo G_{ail}, identification from $u(t)$ to $y(t)$ will provide an estimate biased

by the subsystems G_{ail}, G_C, and C in addition to the various cross-spectra of $v(t)$, $v_{\mathrm{ail}}(t)$, and $v_C(t)$. As before, however, the reference signal $r(t)$ is uncorrelated with the noise signals and may be used as an instrument $\xi(t) = r(t)$ to provide unbiased results.

The cross-covariance function estimate $R_{ur}(\tau)$ for the differential aileron experiment was very similar to Figure 3. Sample signals of the differential aileron experimental data are shown in Figure 11. The signals shown are (1) lateral acceleration at the nose, (2) acceleration at the right forward wing-tip, (3) axial acceleration at the right outer-wing, (4) acceleration at the right aft wing-tip, (5*) acceleration at the right-aft wing-root, (6*) dynamic pressure at the right top front pressure tap, (7) dynamic pressure at the right top rear pressure tap. The same coherence-based criteria of the LEF experiment was used to determine which signals were acceptable for identification purposes; signals marked by '*' were designated unacceptable and not used in the identification algorithm.

Locations of all used and unused accelerometers are shown in Figure 12. Observe that the usable accelerometers are distributed primarily over the wings as one would expect from a differential aileron excitation. The selected accelerometer in the nose measures lateral motion, explaining its high coherence with the OBES signal.

A linear, state-space, discrete-time model was again constructed from the measured data using the method proposed in Section II. The singular values of the projected data matrix (14) are shown in Figure 13. The system order was chosen to be $n = 10$, which is naturally larger than that of the LEF experiment due to the increase in the output dimension n_y. Additionally, the ailerons have much more inertial excitation than the LEF's, being heavier and a larger geometric proportion of the wings, so more responsiveness is expected overall.

Time-domain simulations are plotted with measured data in Figure 14, and comparisons with cross-covariance function estimates in Figure 15. The enumeration is the same as in Figure 11, and the previous comment about the units of the covariance function estimates applies for this example as well.

As a final aside, we mention that the algorithm is capable of analyzing data from multiple inputs and references and would, in theory, provide similar results were the two experiments combined into a single experiment. Data for such an experiment, however, is currently unavailable to the authors.

IV.   Conclusion

We have presented a novel subspace identification algorithm that produces accurate, unbiased, linear models from measured data of large signal dimension (ie. data acquired from many sensors). The algorithm employs covariance function estimates, uses a dynamic-invariance property of the output signals with a strong relationship to classical realization
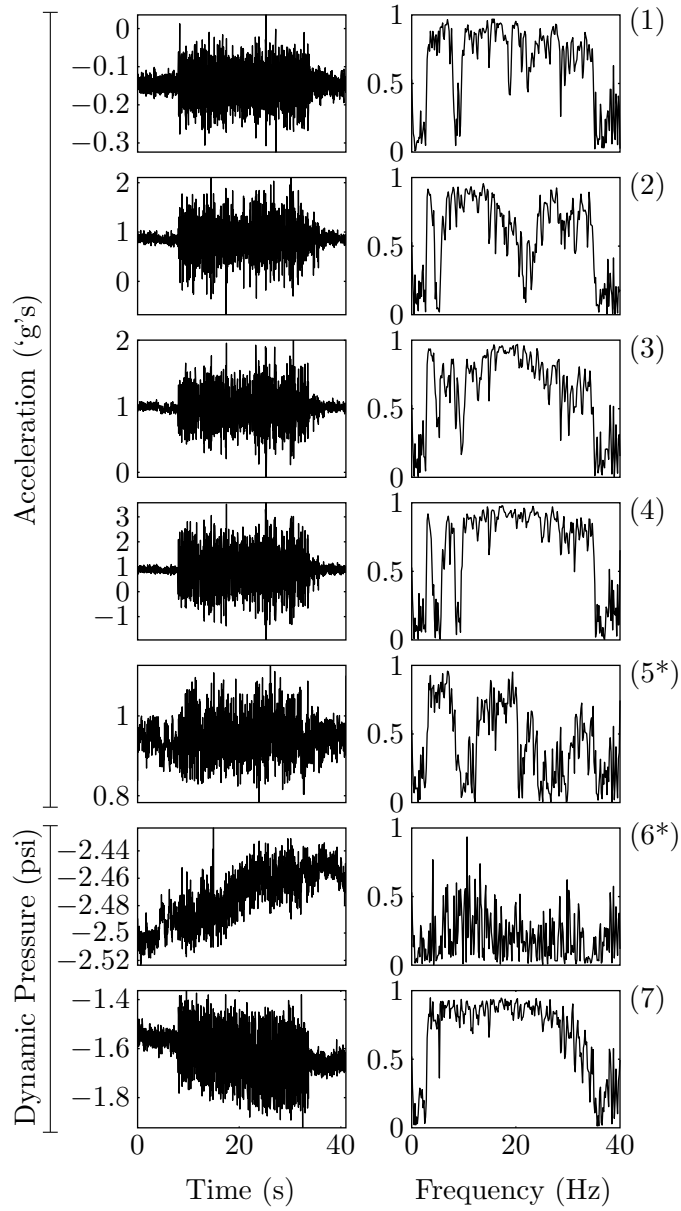
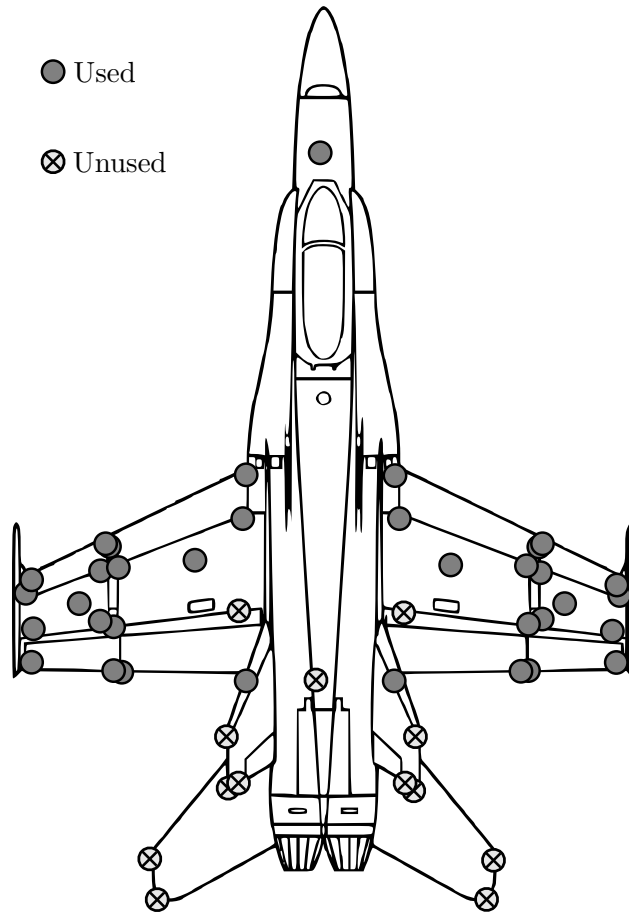Figure 11. Sample of signals used for the differential aileron experiment.

Figure 12. Locations of used and unused accelerometers for the differential aileron experiment.
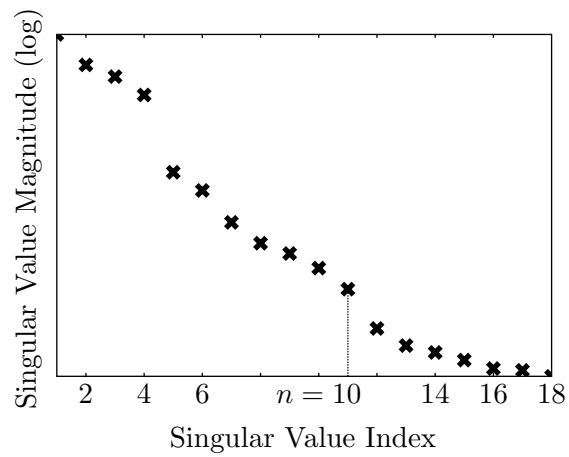

Figure 13. Singular values of the projected data matrix for the differential aileron experiment.
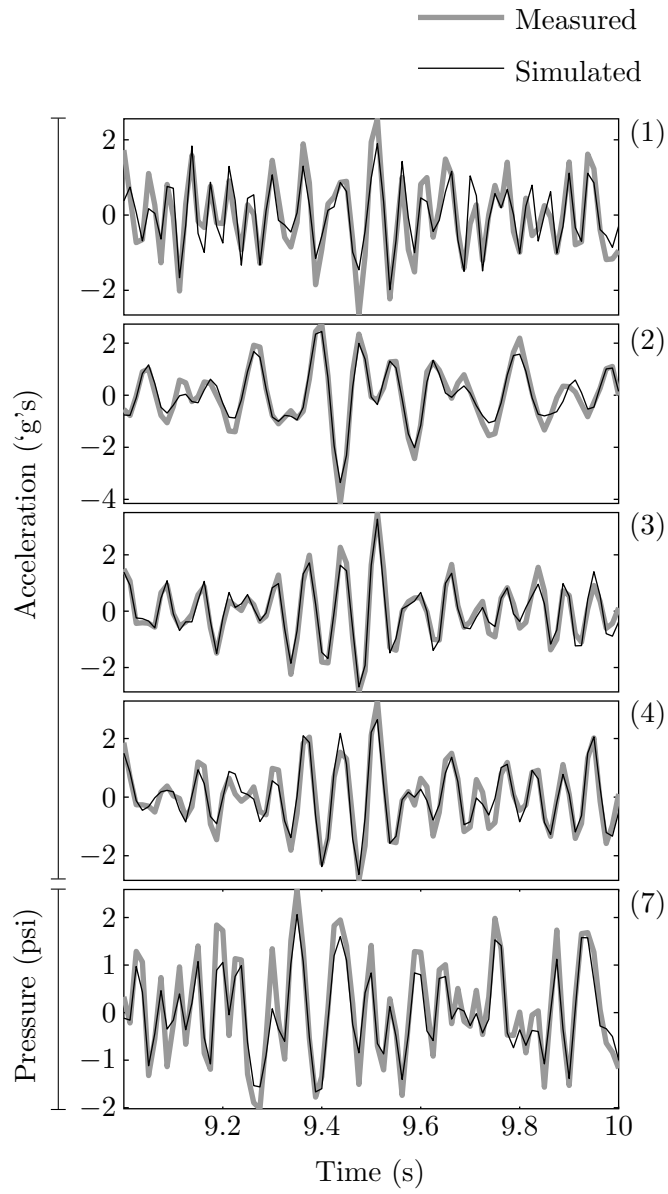
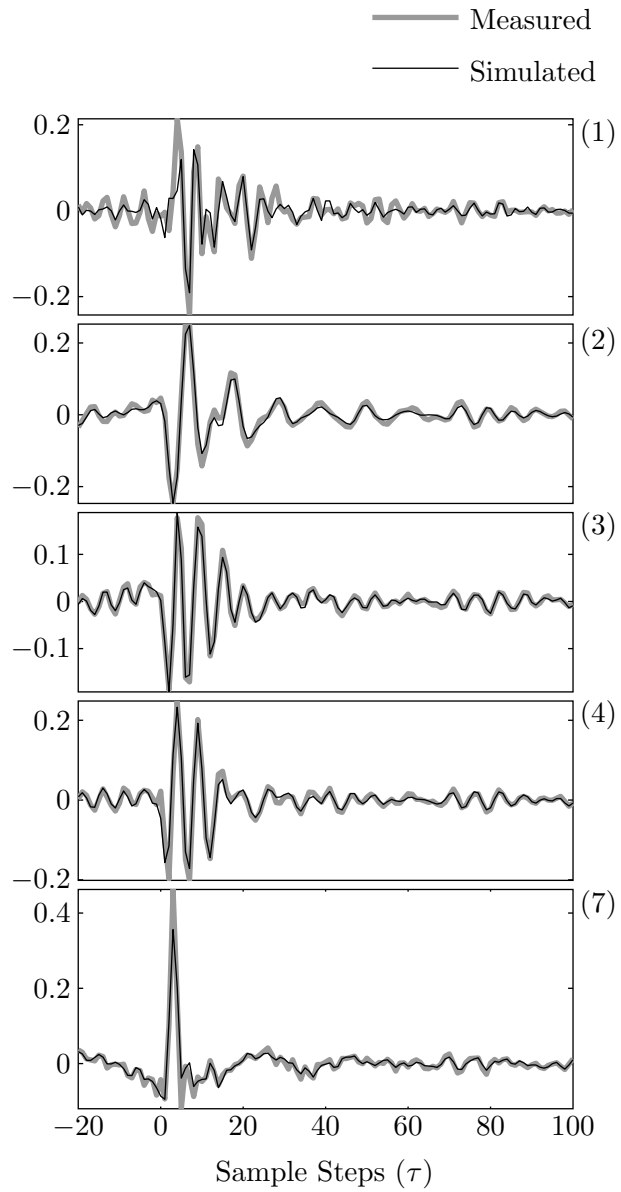**Figure 14. Sample of simulation results of the differential aileron experiment.**

Figure 15. Sample of simulation cross-covariance estimates of the differential aileron experiment.

theory, and relies exclusively on reliable numerical linear algebra techniques and requires no iterative solution. The convergence of covariance function estimates is used to handle large data sets in both open- and closed-loop experiments. The algorithm has been successfully applied to data measured in flight from the NASA Active Aeroelastic Wing F/A-18 for both open-loop and closed-loop experiments.

References

[1]Brenner, M. J., Lind, R. C., and Voracek, D. F., "Overview of Recent Flight Flutter Testing Research at NASA Dryden," Tech. rep., NASA Dryden Flight Research Center, Edwards, California, 1997.

[2]Van Overschee, P. and De Moor, B., "A Unifying Theorem for Three Subspace System Identification Algorithms," *Automatica*, Vol. 31, No. 12, Dec. 1995, pp. 1853–1864.

[3]Mehra, R., Mahmood, S., and Waissman, R., "Identification of Aircraft and Rotorcraft Aeroelastic Modes Using State Space System Identification," *Proceedings of the 4th IEEE Conference on Control Applications*, IEEE, 1995, pp. 432–437.

[4]Mevel, L., Goursat, M., Benveniste, A., and Basseville, M., "Aircraft Flutter Test Design Using Identification and Simulation: a SCILAB Toolbox," *Proceedings of 2005 IEEE Conference on Control Applications*, IEEE, Toronto, Canada, 2005, pp. 1115–1120.

[5]Mevel, L., Benveniste, A., Basseville, M., Goursat, M., Peeters, B., Van der Auweraer, H., and Vecchio, A., "Input/output versus output-only data processing for structural identificationApplication to in-flight data analysis," *Journal of Sound and Vibration*, Vol. 295, No. 3-5, Aug. 2006, pp. 531–552.

[6]Katayama, T., *Subspace Methods for System Identification*, Communications and Control Engineering, Springer-Verlag, 2005.

[7]Miller, D. N. and de Callafon, R. A., "Subspace Identication Using Dynamic Invariance in Shifted Time-Domain Data," *Proceedings of the 50th IEEE Conference on Decision and Control*, Atlanta, GA, USA, 2010.

[8]Verboven, P., Cauberghe, B., Guillaume, P., Vanlanduit, S., and Parloo, E., "Modal parameter estimation and monitoring for on-line flight flutter analysis," *Mechanical Systems and Signal Processing*, Vol. 18, No. 3, 2004, pp. 24.

[9]Baldelli, D. H., Zeng, J., Lind, R. C., and Harris, C., "Flutter-Prediction Tool for Flight-Test-Based Aeroelastic Parameter-Varying Models," *Journal of Guidance, Control, and Dynamics*, Vol. 32, No. 1, Jan. 2009, pp. 158–171.

[10]Juang, J.-N. and Pappa, R. S., "An Eigensystem Realization Algorithm (ERA) for Modal Parameter Identification and Model Reduction," *JPL Proc. of the Workshop on Identification and Control of Flexible Space Structures*, Vol. 3, April 1985, pp. 299–318.

[11]Juang, J.-N., Phan, M. Q., Horta, L. G., and Longman, R. W., "Identification of Observer/Kalman Filter Markov Parameters: Theory and Experiments," *Journal of Guidance, Control, and Dynamics*, Vol. 16, No. 2, 1993, pp. 320–329.

[12]Ljung, L., *System Identification: Theory for the User*, PTR Prentice Hall Information and System Sciences, Prentice Hall PTR, Upper Saddle River, NJ, 2nd ed., 1999.

[13]Chen, C.-T., *Linear System Theory and Design*, Oxford University Press, 1st ed., 1984.

[14]Willems, J., Rapisarda, P., Markovsky, I., and De Moor, B., "A note on persistency of excitation," *Systems & Control Letters*, Vol. 54, No. 4, April 2005, pp. 325–329.

[15]Golub, G. and Van Loan, C., *Matrix Computations*, The Johns Hopkins University Press, 3rd ed., 1996.

[16]Miller, D. N. and de Callafon, R. A., "Efficient Identification of Input Dynamics for Correlation Function-Based Subspace Identification," *18th IFAC World Congress (to appear)*, 2011.

[17]Van Overschee, P. and De Moor, B., *Subspace Identification for Linear Systems: Theory, Implementation, Applications*, Kluwer Academic Publishers, 1996.

[18]Verhaegen, M. and Verdult, V., *Filtering and System Identification: A Least Squares Approach*, Cambridge University Press, 1st ed., May 2007.

[19]Viberg, M., Wahlberg, B., and Ottersten, B., "Analysis of state space system identification methods based on instrumental variables and subspace fitting," *Automatica*, Vol. 33, No. 9, Sept. 1997, pp. 1603–1616.

[20]The Mathworks, "Matlab System Identification Toolbox," 2009.

[21]Chou, C. and Verhaegen, M., "Subspace Algorithms for the Identification of Multivariable Dynamic Errors-in-Variables Models," *Automatica*, Vol. 33, No. 10, Oct. 1997, pp. 1857–1869.

[22]Kung, S. Y., "A new identification and model reduction algorithm via singular value decomposition," *Proceedings of the 12th Asilomar Conference on Circuits, Systems, and Computers*, 1978, pp. 705–714.

[23]Pintelon, R. and Schoukens, J., *System Identification: A Frequency Domain Approach*, Wiley-IEEE Press, Jan. 2001.